

Ab initio study of SrTiO₃ surfaces

J. Padilla, David Vanderbilt *

Department of Physics and Astronomy, Rutgers University, 136 Frelinghuysen Road, Piscataway, NJ 08854-8019, USA

Received 18 February 1998; accepted for publication 17 August 1998

Abstract

We present first-principles total-energy calculations of (001) surfaces of SrTiO₃. Both SrO-terminated and TiO₂-terminated surfaces are considered, and the results are compared with previous calculations for BaTiO₃ surfaces. The major differences are in the details of the relaxed surface structures. Our calculations argue against the existence of a large ferroelectric relaxation in the surface layer, as had been previously proposed. We do find some indications of a weak surface ferroelectric instability, but so weak as to be easily destroyed by thermal fluctuations, except perhaps at quite low temperatures. We also compute surface relaxation energies and surface electronic band structures, obtaining results that are generally similar to those for BaTiO₃. © 1998 Elsevier Science B.V. All rights reserved.

Keywords: Density functional calculations; Dielectric phenomena; Surface energy; Surface relaxation and reconstruction

1. Introduction

The cubic perovskites are an important class of materials that are of particular interest because of the variety of structural phase transitions that they display [1]. The structural instabilities may be of ferroelectric (FE) character, as for BaTiO₃, or of antiferrodistortive character (involving rotation of oxygen octahedra), as for SrTiO₃. Specifically, SrTiO₃ adopts a paraelectric simple cubic perovskite structure above $T_c = 105$ K, but transforms to a tetragonal antiferrodistortive structure below T_c ; and while it shows strong signs of FE fluctuations at very low temperature, it evidently remains paraelectric down to zero temperature.

The (001) and (111) surfaces of cubic perovskites have been most investigated experimentally

[2]. For a II–IV perovskite such as SrTiO₃, there are two possible non-polar (001) surface terminations: a SrO-terminated surface (type I), and a TiO₂-terminated surface (type II). On the other hand, the (111) surfaces are polar, and therefore presumably much less stable. Here we focus on the (001) surfaces of SrTiO₃.

Interest in the surface properties of SrTiO₃ arises because of the catalytic properties of these surfaces [3], and because of the common use of SrTiO₃ as a substrate for epitaxial growth of high T_c superconductors (such as YBa₂Cu₃O₇) [4] and other oxides.

Theoretical studies of these surfaces have been numerous. Wolfram et al. [5], using a linear combination of atomic orbitals approach, predicted mid-gap surface states for SrTiO₃, in disagreement with experimental investigations [6,7]. Tsukada et al. [8] employed the DV X α cluster method to study SrTiO₃ surfaces, finding no mid-gap surface states.

* Corresponding author. E-mail: dhv@physics.rutgers.edu

However, cluster methods are not very suitable for high-accuracy calculations of relaxations and electronic states on infinite surfaces, underlining the need for the application of more accurate, self-consistent techniques. First-principles density-functional calculations have been very successful in the study of bulk perovskites [9–15], and more recently there have been similar calculations for perovskite surfaces [16–19]. In particular, Kimura et al. [19] applied the same method as in this paper, the plane-wave ultrasoft pseudopotential method [20], to the study of (001) surface of SrTiO₃, with and without oxygen vacancies at the surfaces. The main difference between that report and the present work is that we fully relax the atomic coordinates in the slab. Also, we analyze the possible existence of a FE surface layer for the SrO surface [21], as has been suggested previously.

On the experimental side, the study of these surfaces is complicated by the presence of surface defects [22], making it difficult to verify the surface stoichiometry. The results also tend to depend upon the surface treatment [23]. Low-energy electron diffraction (LEED) and reflection high-energy electron diffraction (RHEED) studies of SrTiO₃ surfaces have been reported [23–27]. Some of them show no reconstruction of the surface layer [23–25]. In contrast, others [26,27], as well as photoelectron spectroscopy [28] and scanning tunneling microscopy [29] observations, show different reconstructions for the reduced surfaces. The absence of in-gap surface states has also been shown [6].

2. Theoretical approach

As in previous work on BaTiO₃ surfaces [16], we employ here a self-consistent pseudopotential technique in which the valence electron wave functions are obtained by minimizing the Kohn–Sham total-energy functional using a conjugate-gradient technique [30]. The exchange-correlation potential is treated within the local-density approximation (LDA) in the Ceperley–Alder form [31]. Vanderbilt ultrasoft pseudopotentials [20] are used to avoid norm-conservation constraints, thus permitting the use of a small plane-wave cut-off of

25 Ry, in spite of the fact that we are dealing with first-row and transition metal atoms. Such a cut-off has previously been shown to be adequate in the bulk [30]. The forces on each ion were relaxed to less than 0.02 eV/Å using a modified Broyden scheme [32].

Our calculations are carried out in a periodic slab geometry. For the type I (SrO-terminated) surface, the slab contains 17 atoms (four SrO layers and three TiO₂ layers). Similarly, the type II (TiO₂-terminated) slab contains 18 atoms (four TiO₂ layers and three SrO layers). In both cases, the slabs were thus three lattice constants thick; the vacuum region was two lattice constants thick. The *z*-axis is taken as normal to the surface. The calculations were done with a (6, 6, 2) Monkhorst–Pack mesh [33]. This *k*-point set produced results of very good accuracy. The structure was set up using our theoretical lattice constant of 3.86 Å, which is about 1% smaller than the experimental one; this underestimation is typical of LDA calculations. For further details concerning our method and its accuracy, we direct the reader to our earlier paper [16].

Below 105 K, SrTiO₃ transforms to a tetragonal antiferrodistortive (AFD) state in which the oxygen octahedra rotate about a $\langle 001 \rangle$ axis in opposite directions in alternate unit cells [34]. However, these rotations are typically small; even at $T=0$ they amount to only $\sim 3^\circ$. Since we are mainly interested in comparing with room temperature experiments, and since the static AFD distortions have already disappeared at 105 K (well below room temperature), we have not included them in our calculations. On the other hand, we do not want to consider the possible presence of a FE surface layer, as suggested in ref. [21].

We thus chose symmetries as follows. Most of the calculations were carried out using a “full set” of symmetries, consisting of M_x , M_y , and M_z mirror symmetries (the latter being a reflection through the center plane of the slab), as well as 1×1 translational symmetries parallel to the surface. The full set of symmetries prevents the occurrence of FE as well as AFD distortions. Then, some further calculations were carried out using a “reduced set” of symmetries, identical to the full set except that M_x symmetry is allowed to be

broken. The reduced set of symmetries, while still suppressing the AFD instability, allows the surface to develop a FE distortion along \hat{x} if it should turn out to be energetically favorable.

3. Surface relaxations

We begin by presenting the relaxed structure for each of the two surface terminations, obtained by starting from the ideal structure and then relaxing the atomic positions while preserving the full set of symmetries. The relaxed geometries are summarized in Table 1. (Coordinates are only listed for atoms in the top half of the slab, $z \geq 0$; the others are determined by M_z mirror symmetry.) By symmetry, there are no forces along \hat{x} or \hat{y} . To set notation, oxygen atoms O_I are the ones lying in SrO planes of the slab, while O_{II} refers to the oxygen atoms lying in TiO_2 planes of the slab. The layer numbering in Table 1 is from the outermost layer inwards.

From Table 1, we can see the largest relaxations are for the metal atoms in the surface layer, -5.7% and -3.4% for the Sr-terminated and Ti-terminated surfaces, respectively. The outward relaxation of the second-layer Sr atom on the Ti-terminated surface is also noteworthy. The surface-layer oxygen atoms show almost no displacement on the Sr-terminated surface.

Previous surface structural refinements have been carried out by Bickel et al. [24,25] and by Hikita et al. [23] using (LEED) and (RHEED),

Table 1
Equilibrium atomic displacements (relative to ideal positions) for the SrO- and TiO_2 -terminated surfaces, when no symmetry-breaking distortions are allowed. Units are relative to the theoretical lattice constant ($a = 3.86 \text{ \AA}$)

Layer	SrO surface	δz	TiO_2 surface	δz
1	Sr	-0.057	Ti	-0.034
	O_I	0.001	O_{II}	-0.016
2	Ti	0.012	Sr	0.025
	O_{II}	0.	O_I	-0.005
3	Sr	-0.012	Ti	-0.007
	O_I	-0.001	O_{II}	-0.005

Table 2

Comparison of theoretical and experimental structural parameters for symmetry-preserving surface relaxations. Δd_{12} and Δd_{23} are respectively the changes in interlayer spacing for the first and second pair of layers, while s measures the outward displacement of the surface oxygens relative to the first-layer metal atoms. All quantities are in angstroms

	s	Δd_{12}	Δd_{23}
<i>SrO-terminated</i>			
Theory, present	0.22	-0.26	0.10
Theory, ref. [35]	0.14	-0.47	
Exp., refs. [24,25]	0.16	-0.19	0.08
Exp., ref. [23]	0.16	0.10	0.05
<i>TiO₂-terminated</i>			
Theory, present	0.07	-0.27	0.12
Theory, ref. [35]	0.04	-0.39	
Exp., refs. [24,25]	0.08	0.04	-0.04
Exp., ref. [23]	0.10	0.07	0.05

respectively. In Table 2, we compare our structural parameters with the two experimental ones. Both experimental groups assumed that the oxygen and metal atoms remain coplanar in the second and third layers in order to simplify the refinement procedure; since the scattering strength of O is much smaller than that of Sr and Ti [24,25], our theoretical comparison is made to the position of the subsurface metal layers. Thus, we define Δd_{12} as the change (relative to bulk) of the first interlayer spacing, as measured from the surface to the subsurface metal z -coordinate, and similarly for Δd_{23} . The quantity s measures the outward displacement of the surface-layer oxygens relative to the surface-layer metal atoms.

It is evident that the agreement between the theory and the experimental refinements is not very good. This is not surprising in view of the fact that the experimental structures are in poor agreement with each other (while a statement appears in ref. [23] to the effect that their results are “basically consistent” with those of refs. [24,25], this statement is not supported by a direct comparison of the two sets of results, as in Table 2). Our values for the rumpling of s of the surface layer are in rough qualitative agreement with the experimental ones, though somewhat larger in magnitude. However, we predict a sub-

stantial contraction of the interlayer spacing d_{12} , while in most cases the experimental refinement indicates an expansion instead. The one exception is for the Sr-terminated surface, where our theory is in reasonable agreement with refs. [24,25], although not with ref. [23]. The agreement for the second interlayer spacing can be seen to be mixed.

The disagreement between the two sets of experimental numbers suggests that the experimental refinements should perhaps not be taken too seriously. The expected quality of a LEED or RHEED refinement is not well established for a complicated metal oxide surface such as this one. In the work of Bickel et al. [24,25], the authors were not able to determine independently the proportions of the surface exhibiting the SrO and TiO₂ terminations; they assumed that the two appear in equal proportions. Refining the structural parameters for both simultaneously, they then obtained an R -factor of 0.53. While this was argued to be “acceptable in view of the complexity of the structure”, it nevertheless seems uncomfortably large. In the work of Hikita et al. [23], the surface was prepared under different conditions in order to obtain SrO and TiO₂ terminations separately; for these, R -factors of 0.28 and 0.26 were obtained, respectively. While this would thus appear to be the more reliable experiment, unfortunately it is in no better agreement with the theory than for the refinement of refs. [24,25]. One possible problem with both experimental refinements could be the arbitrary assumption that there is no buckling in the second metal–oxygen plane. Our results indicate that there is a substantial buckling in that layer, especially in the case of the subsurface SrO layer on the TiO₂-terminated surface.

Also included in Table 2 are theoretical estimates of Mackrodt [35] using an interatomic potential based on Kim–Gordon pair potentials. This theory gives results that are qualitatively similar to ours, although the pair-potential model appears to overestimate the size of the interlayer relaxations and underestimate the degree of surface rumpling. The pair-potential model also predicts a significant rumpling in the subsurface SrO layer of the TiO₂-terminated surface, similar to what we reported above in Table 1.

4. Testing for a ferroelectric monolayer

Bulk SrTiO₃ is an incipient ferroelectric: it nearly becomes ferroelectric at very low temperature, and is apparently prevented from doing so only by quantum zero-point fluctuations [36]. In our work on surfaces of FE BaTiO₃, we found some tendency for an enhancement of the FE order in the first few surface layers, especially for the case of the TiO₂ termination. Thus, it is intriguing to speculate that if a similar tendency exists in SrTiO₃, it might lead to the formation of a FE surface layer on top of a paraelectric bulk material, at least at low temperatures. In fact, the presence of just this kind of FE monolayer at the surface has been predicted by Ravikumar et al. [21] for the SrO termination of SrTiO₃. However, this prediction is based on an empirical interatomic potential developed for ionic systems, and it is not clear how far such a pair-potential approach can be trusted for deciding such a delicate question as the appearance of surface FE order. Thus, we have undertaken to check whether such a FE surface phase might occur in the context of our *ab initio* calculations.

Note that while Bickel et al. have discussed the rumpling of the surface layer in terms of a “ferroelectric relaxation” normal to the surface [24,25], such a rumpling does not break any symmetry of the ideal surface, and is not qualitatively different from the rumpling observed on other oxide surface. Thus, when we speak of a FE surface layer, we shall restrict ourselves here to symmetry-breaking distortions, i.e. frozen-in displacements parallel to the surface. Indeed, Ravikumar et al. predict enormous displacements of this kind for the SrO-terminated surface: Sr and O shift by 0.43 Å and –0.33 Å, respectively, along a $\langle 100 \rangle$ direction, with a resulting reduction in surface energy of 0.11 eV/cell. When the primitive 1×1 periodicity of the surface cell is allowed to be broken, they find an even lower energy $c2 \times 2$ structure.

With this motivation, we have investigated carefully the stability of our 1×1 surface with respect to displacements of the surface atoms along the x -axis, using the reduced set of symmetries as discussed in Section 2. Starting from the structure of Table 1, an additional FE distortion along \hat{x} is

imposed, the value of this distortion being taken the same as for bulk BaTiO_3 as computed in ref. [30]. Then we allow this structure to relax fully. We did these simulations for both kinds of termination, and for both theoretical and experimental lattice constants.

For the case of experimental lattice constant, the resulting displacements along the \hat{x} direction, in units of lattice constant, are as follows. For the SrO-terminated surface, the first- and third-layer Sr displacements are 0.005 and 0.006; the second- and fourth-layer Ti displacements are 0.005 and 0.008; and the oxygen displacements are -0.007 , -0.002 , -0.006 , and -0.004 in layers 1 through 4, respectively. For the TiO_2 -terminated surface, the first- and third-layer Ti displacements are 0.017 and 0.016; the second- and fourth-layer Sr displacements are 0.010 and 0.011; and the oxygen displacements are -0.011 , -0.008 , -0.007 , and -0.009 in layers 1 through 4, respectively. The total energies lie below those of the high-symmetry structure (i.e. no \hat{x} distortion) by 0.001 by 0.026 eV for the SrO- and TiO_2 -terminated surfaces, respectively. We see that the final FE distortions left after the relaxations are indeed very small, and are not much greater in the surface layer than in the deeper layers. When using the theoretical lattice constant instead of the experimental one, we found only a very weak distortion of energy 0.001 eV for the TiO_2 -terminated case, and no observable distortion for the SrO-terminated case.

These results indicate that there does exist the possibility of a small FE surface distortion for both surface terminations of SrTiO_3 . However, the double-well depth that we found for the SrO surface is very much smaller than the one predicted by Ravikumar et al. [21]. We actually find a somewhat larger tendency for FE distortion for the TiO_2 surface, but still the distortion amplitudes (maximum 0.07 \AA) and energy (0.013 eV/surface) are nearly an order of magnitude smaller than the SrO surface prediction of ref. [21]. Our predicted FE distortion is small enough that it may easily be destroyed by thermal (or even quantum) fluctuations, and it seems unlikely that it would appear at room temperature. However, it seems possible that the FE distortion might survive and be observable at very low temperatures.

5. Surface energies

We discuss next the surface energetics. To compare energies of surfaces having different stoichiometry, we follow the approach described in ref. [16]. That is, we consider each surface slab to be built from TiO_2 and SrO units, and compute the grand thermodynamic potential F for each type of surface as a function of the TiO_2 chemical potential μ_{TiO_2} . The energies of the bulk crystals of SrO and TiO_2 were calculated with the LDA using the same pseudopotentials, and the same plane-wave cut-off. The final results are shown in Fig. 1. It can be seen that both surfaces have a comparable range of thermodynamic stability, indicating that either termination could be formed depending on whether growth occurs in Sr-rich or Ti-rich conditions, with a very small preference for the TiO_2 termination.

The average of F for the two types of surface, which we shall denote as E_{surf} , is independent of μ_{TiO_2} . Thus, this quantity is convenient for comparisons. The value we found for E_{surf} for the $\text{SrTiO}_3(001)$ surfaces is 1.26 eV per surface unit cell (1358 erg/cm^2). This is very similar to the corresponding value of 1.24 eV that was obtained for the $\text{BaTiO}_3(001)$ surfaces (in the cubic phase).

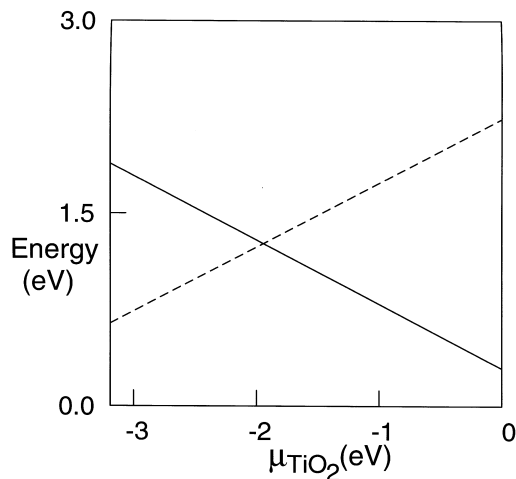


Fig. 1. Grand thermodynamic potential F as a function of the chemical potential μ_{TiO_2} , for the two types of surfaces. Dashed and solid lines correspond to type I (SrO-terminated) and type II (TiO_2 -terminated) surfaces, respectively.

To compute the surface relaxation energy E_{relax} , we computed the average surface energy E_{unrel} for the unrelaxed slabs (i.e. atoms in the ideal cubic configuration), using the same k -point sampling as for the relaxed systems. We obtained $E_{\text{unrel}} = 1.44$ eV. Thus, the relaxations account for 0.18 eV of the surface energy per surface unit cell, accounting for around 15% of the total surface energy.

6. Surface electronic structure

We focus now on the LDA calculated electronic structure for the surface slabs. Although the LDA is well known to underestimate the band gaps, we can be assured that the results given here are at least qualitatively correct. The band gap we obtained for bulk SrTiO₃ is 1.85 eV, to be compared with the experimental value of 3.30 eV; this level of disagreement is typical for the LDA.

Not surprisingly, our results for the band structures of the surfaces of SrTiO₃ are very similar to the case of BaTiO₃ surfaces [16]. The computed LDA electronic energy band structure is given in Fig. 2 and the direct energy gaps are given in Table 3. We see that the band gap for the SrO surface almost does not change with respect to the bulk value, and no in-gap state occurs. For the TiO₂ surface, there is a substantial reduction of the band gap. However, there are no deep-gap surface states, in accord with experimental reports [6].

From Fig. 2c we see (as is also true for BaTiO₃) [16] that there is a tendency for valence-band states to intrude upwards into the lower part of the band gap for this surface, especially near the M point of the surface Brillouin zone, that is the top of the valence band. In order to analyze the character of the valence-band state at the M point of the TiO₂ surface, the charge density at this state was obtained. The results are very similar to those shown in fig. 4 of ref. [16] for the case of BaTiO₃. These states correspond to O 2p orbitals lying in the surface plane and having very little hybridization with Ti 3d levels because of the existence of four nodal planes [(100), (110), (010), and ($\bar{1}10$)] intersecting at the Ti sites.

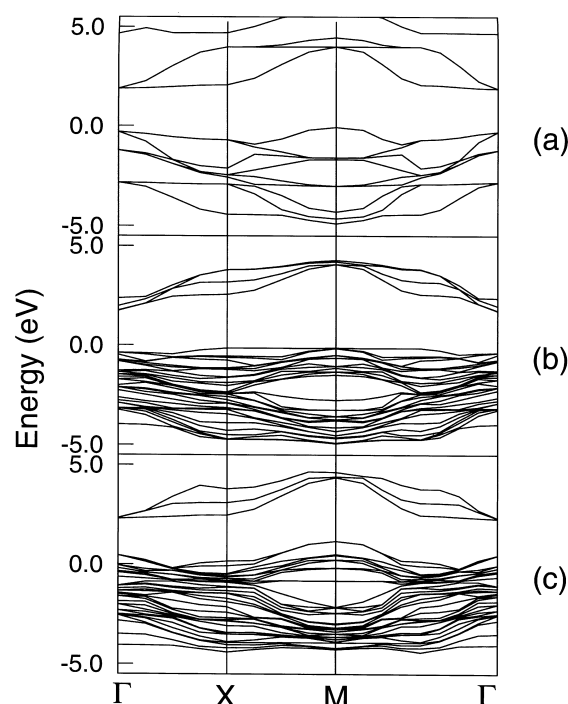


Fig. 2. Calculated electronic band structures for SrTiO₃. (a) Surface-projected bulk band structure. (b) SrO-terminated surface (slab I). (c) TiO₂-terminated surface (slab II). The zero of energy corresponds to the bulk valence band maximum. Only the lowest few conduction bands are shown.

Table 3
Calculated electronic energy band gaps for the relaxed surface slabs (eV)

Slab	Band gap
I	1.86
II	1.13
Bulk	1.85

7. Summary

In summary, we have carried out LDA density-functional calculations of SrO- and TiO₂-terminated (001) surfaces of SrTiO₃. By minimizing the Hellmann–Feynman forces on the atoms, we obtained the optimal ionic positions. Previous experimental LEED [24,25] and RHEED [23] surface structure determinations are found to be significantly at variance with our predictions, as well as with each other.

Our calculations do not support the existence of a large FE distortion in the surface layer of the Sr-terminated surface, as had been previously proposed theoretically [21]. While we cannot rule out a weak FE surface instability, especially for the Ti-terminated surface, our results indicate that it would be sufficiently weak so as to be easily destroyed by thermal fluctuations, except at quite low temperatures. The equilibrium state of the surface was obtained as a function of the relative Sr and Ti stoichiometry. The average energy of the Sr- and Ti-terminated surfaces was found to be ~ 1360 erg/cm², and the surface relaxation energy was calculated to be ~ 190 erg/cm². In agreement with experiments, no deep-gap surface level is found. However, as found for BaTiO₃, there is a significant reduction of the electronic band gap of the TiO₂ surface. This reduction arises from surface states in the lower part of the bulk band gap which can be regarded as resulting from the intrusion of valence-band states of O 2p character, particularly in the vicinity of the *M* point of the surface Brillouin zone.

Acknowledgements

The present work was supported by ONR Grant N00014-97-1-0048 and NSF Grant DMR-96-13648.

References

- [1] M.E. Lines, A.M. Glass, Principles and Application of Ferroelectrics and Related Materials, Clarendon Press, Oxford, 1977.
- [2] V.E. Henrich, P.A. Cox, The Surface Science of Metal Oxides, Cambridge University Press, New York, 1994.
- [3] M. Tomkiewicz, H. Fay, Appl. Phys. 18 (1979) 1.
- [4] P. Chaudhari, R.H. Koch, R.B. Laibowitz, T.R. McGuire, R.J. Gambino, Phys. Rev. Lett. 58 (1987) 2684.
- [5] T. Wolfram, E.A. Kraut, F.J. Morin, Phys. Rev. B 7 (1973) 1677.
- [6] R.A. Powell, W.F. Spicer, Phys. Rev. B 13 (1976) 2601.
- [7] V.E. Henrich, G. Dresselhaus, H.J. Zeiger, Bull. Am. Phys. Soc. Ser. II 22 (1977) 364.
- [8] M. Tsukada, C. Satoko, H. Adachi, J. Phys. Soc. Jpn. 48 (1980) 200.
- [9] W. Zhong, R.D. King-Smith, D. Vanderbilt, Phys. Rev. Lett. 78 (1994) 3618.
- [10] W. Zhong, D. Vanderbilt, K.M. Rabe, Phys. Rev. Lett. 73 (1994) 1861.
- [11] W. Zhong, D. Vanderbilt, K.M. Rabe, Phys. Rev. B 52 (1995) 6301.
- [12] R.E. Cohen, H. Krakauer, Phys. Rev. B 42 (1990) 6416.
- [13] R.E. Cohen, H. Krakauer, Ferroelectrics 136 (1992) 65.
- [14] R.E. Cohen, Nature 358 (1992) 136.
- [15] D.J. Singh, Ferroelectrics 164 (1995) 143.
- [16] J. Padilla, D. Vanderbilt, Phys. Rev. B 56 (1997) 1625.
- [17] R.E. Cohen, J. Phys. Chem. Solids 57 (1996) 1393.
- [18] R.E. Cohen, Ferroelectrics 194 (1997) 323.
- [19] S. Kimura, J. Yamauchi, M. Tsukada, S. Watanabe, Phys. Rev. B 51 (1995) 11059.
- [20] D. Vanderbilt, Phys. Rev. B 41 (1990) 7892.
- [21] V. Ravikumar, D. Wolf, V.P. Dravid, Phys. Rev. Lett. 74 (1995) 960.
- [22] B. Cord, R. Courths, Surf. Sci. 287/288 (1993) 377.
- [23] T. Hikita, T. Hanada, M. Kudo, Surf. Sci. 287/288 (1993) 377.
- [24] N. Bickel, G. Schmidt, K. Heinz, K. Muller, Phys. Rev. Lett. 62 (1989) 2009.
- [25] N. Bickel, G. Schmidt, K. Heinz, K. Muller, Vacuum 41 (1990) 46.
- [26] M. Naito, H. Sato, Physica C 229 (1994) 1.
- [27] K. Kitahama, Q.R. Feng, T. Kawai, S. Kawai, Bull. Fall Meet. Jpn. Appl. Phys. Soc. 2 (1992) 494.
- [28] V.E. Henrich, G. Dresselhaus, H.J. Zeiger, Phys. Rev. B 17 (1978) 4908.
- [29] T. Matsumoto, H. Tanaka, K. Kogouchi, T. Kawai, S. Kawai, Surf. Sci. 312 (1993) 21.
- [30] R.D. King-Smith, D. Vanderbilt, Phys. Rev. B 49 (1994) 5828.
- [31] D.M. Ceperley, B.J. Alder, Phys. Rev. Lett. 45 (1980) 566.
- [32] D. Vanderbilt, S.G. Louie, Phys. Rev. Lett. B30 (1984) 6118.
- [33] H.J. Monkhorst, J.D. Pack, Phys. Rev. B 13 (1976) 5188.
- [34] D. Vanderbilt, W. Zhong, Phys. Rev. Lett. 74 (1995) 2587.
- [35] W.C. Mackrodt, Phys. Chem. Min. 15 (1988) 228.
- [36] W. Zhong, D. Vanderbilt, Phys. Rev. B 53 (1996) 5047.